# The Effect of Infrastructure Removal on Cycling Activity

Carol Sobral

December 22, 2025*

## 1 Introduction

Urban transport policy in European cities has become increasingly contested, particularly around the reallocation of road space from motor vehicles to bicycles and pedestrians [1, 2]. While a growing empirical literature examines whether the construction of cycling infrastructure increases cycling activity [3–5], less is known about the causal effects of removing it.

My goal with this project is to exploit a court-mandated removal of infrastructure in Berlin to estimate the causal effect of the loss of dedicated cycling space on cycling activity. In August 2020, the Berlin Senate closed a 500-meter section of Friedrichstraße—a central north–south arterial road—to private motor vehicles and introduced a pedestrian zone with painted cycling lanes. On November 21, 2022, a court ruling reverted the street to its original configuration, with cycle lanes removed entirely.

I aim to address two questions: (1) What is the causal effect of removing cycling infrastructure on cycling activity, and does it persist over time? (2) If cycling declines, to what extent do trips redirect to adjacent streets versus disappear through mode substitution or trip suppression?

*Apologies for the delay, I'm on Brazil time :)

# 2 Methods

## 2.1 Data

Cycling activity data comes from Strava Metro, which provides anonymized, aggregated GPS-based trip counts per street segment. Prior work shows that Strava trip counts closely track temporal variation in cycling activity, even when user composition is not representative of the population [6, 7].

I aggregate raw trips into weekly counts within fixed hexagonal cells of 500-meter radius (area $\approx 0.65$ km$^2$) that cover the central Berlin road network. The analysis period runs from November 2021 to November 2024.[1] The use of symmetric pre- and post-treatment windows (November–November) reduces sensitivity to seasonal confounding in travel behavior [8].

## 2.2 Research Design and Estimand

The analysis exploits a single treated location observed over time, along with a large set of untreated locations. The estimand of interest is the effect of removing cycling infrastructure on cycling activity in the treated cell. This effect is defined as the difference between observed post-treatment cycling activity and the counterfactual activity that would have prevailed in the absence of the intervention.

Identification relies on the ability of untreated locations to reproduce the pre-treatment outcome trajectory of the treated unit. The counterfactual is constructed as a weighted combination of untreated cells whose pre-treatment cycling patterns closely resemble those of the treated cell.

## 2.3 Synthetic Control

This data structure motivates the use of the synthetic control method [9], which estimates a counterfactual for the treated unit as a weighted average of control units that reproduces the treated unit's pre-treatment outcome trajectory. Let $Y_{1t}$ denote cycling activity in the treated cell and $Y_{jt}$ activity in control cell $j \in \mathcal{J}$. The synthetic control counterfactual is

[1] The pre-treatment period begins after the COVID-19 lockdowns in Germany, to limit the influence of pandemic-related disruption on baseline cycling trends.

given by

$$\hat{Y}_{1t}^{(0)} = \sum_{j \in \mathcal{J}} w_j Y_{jt}, \tag{1}$$

where the weights $w_j \geq 0$ sum to one and are selected to minimize discrepancies between treated and synthetic outcomes in the pre-treatment period.

For the analysis, I use the augmented synthetic control method [10] in a setting with fine spatial units and pronounced seasonal variation, where convex weighting alone may not reproduce the pre-treatment outcome path. The method extends the classical synthetic control weights with a regularized adjustment, such that the counterfactual weights can be written as

$$w = w_{\text{scm}} + w_{\text{aug}}, \tag{2}$$

where $w_{\text{scm}}$ are the weights obtained from the classical synthetic control estimator and $w_{\text{aug}}$ is an augmentation derived from outcome modeling. The magnitude of the augmentation is controlled by a ridge penalty parameter selected via cross-validation.

The counterfactual is constructed using only pre-treatment outcome trajectories, without additional covariates. Treatment effects are estimated as the difference between observed cycling activity and the augmented synthetic counterfactual, computed weekly to assess both immediate impacts and persistence.

### 2.4 Sample

The treated unit is the hexagonal cell containing the affected Friedrichstraße segment. The initial donor pool consists of 1,244 cells that cover the central Berlin road network. Cells that experienced cycling infrastructure changes or related traffic interventions during the study period are excluded from the donor pool to avoid contamination. I also restrict the donor pool to cells with cycling activity recorded in at least 40% of weeks during the analysis period. Finally, the six immediately adjacent cells are held out for examination of potential displacement effects and are not used in constructing the synthetic control. After applying these restrictions, the donor pool contains 1,034 cells.

### 2.5 Inference

I assess statistical significance using placebo tests that reassign treatment to donor cells and compare the treated unit's post-treatment gap to the resulting distribution of placebo

gaps. Placebos with poor pre-treatment fit, defined as having a pre-treatment root mean squared prediction error (RMSPE) exceeding five times that of the treated unit, are excluded.

# 3 Preliminary Results

## 3.1 Pre-Treatment Fit and Diagnostics

The synthetic control achieves a good pre-treatment fit, with an RMSPE of 127.92 trips per week (2.16% of the pre-treatment mean). Visual inspection shows that the synthetic control approximates the treated unit trajectory on average (Figure 1, panel A). For comparison, corresponding diagnostics based on the classical synthetic control estimator are reported in Appendix A.

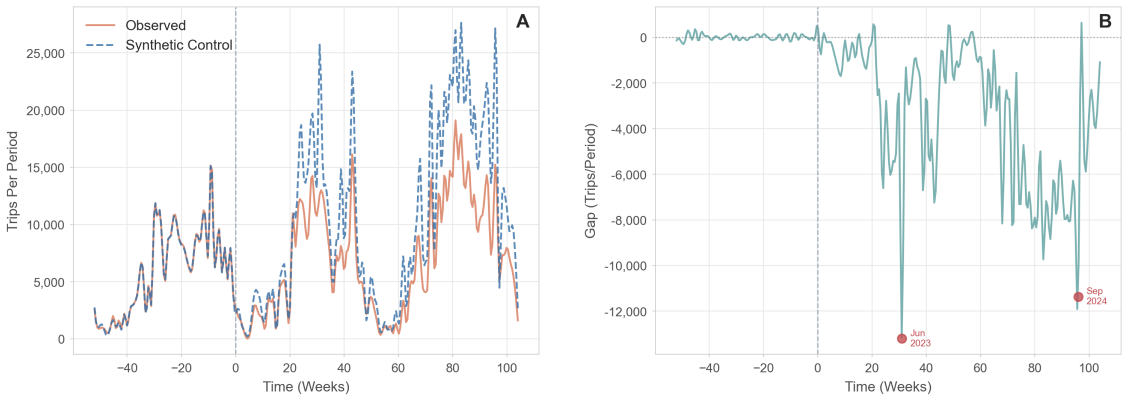


**Figure 1:** Observed and synthetic cycling activity in the treated hexagonal cell. Panel A shows weekly observed cycling trips and the synthetic control. Panel B plots the corresponding gap between observed and synthetic outcomes. The vertical dashed line marks the treatment date.

## 3.2 Treatment Effects

Post-treatment, cycling volumes in Friedrichstraße decline sharply relative to the augmented synthetic counterfactual. The average treatment effect is a reduction of 3,420.96 trips per week, representing a 57.76% decreas compared to average pre-treatment cycling activity (Figure 1, panel B). The effect appears immediately after the intervention and persists throughout the post-treatment period. The largest absolute declines occur in Week 31 (June 2023), with a gap of 13,202 trips, and in Week 96 (September 2024), with a gap of 11,360 trips, suggesting that the treatment effects persist over time.

Appendix B reports the spatial distribution of donor units and descriptive statistics of the highest-weight donors.

### 3.3 Placebo Inference

Figure 2 shows placebo gap trajectories for the donor units that passed the pre-treatment fit threshold (n = 40). The treated unit has a post-treatment RMSPE of 4,618.82, compared to a mean placebo RMSPE of 195.97, resulting in an RMSPE ratio of 36.11. None of the 40 placebo units have post-treatment RMSPE values exceeding that of the treated unit (placebo p-value < 0.025).

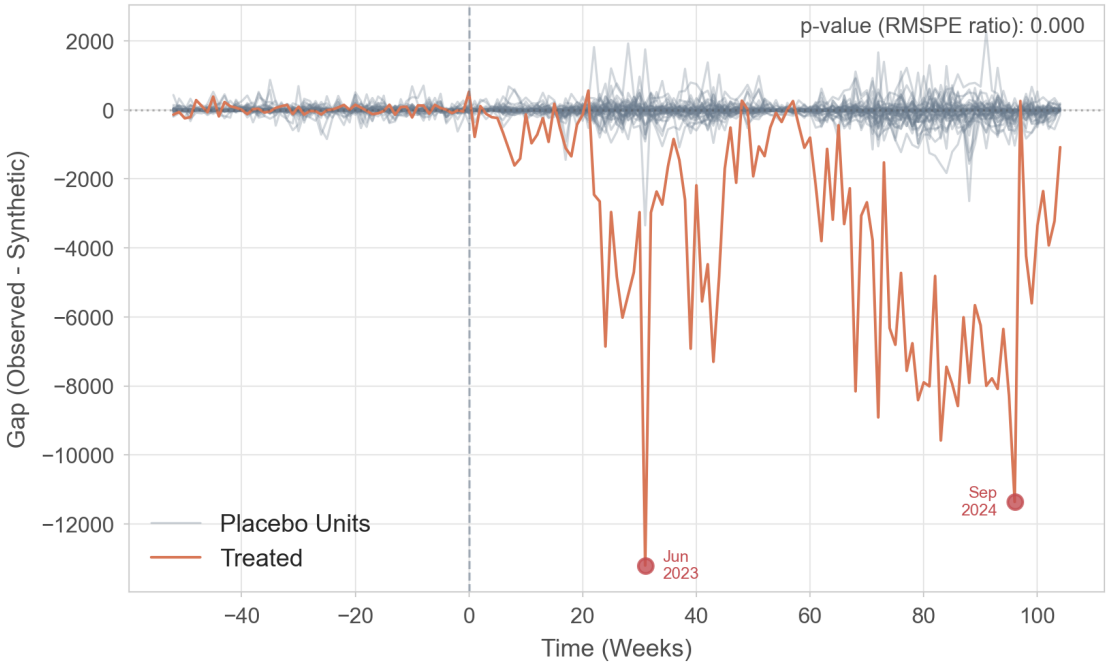


**Figure 2:** Placebo gap trajectories obtained by reassigning treatment to donor units. Grey lines indicate placebo gaps for donor units treated on the same intervention date; the orange line indicates the treated unit. The vertical dashed line marks the treatment date.

## 4 Next Steps

The final analysis will assess the robustness of the estimated treatment effects using standard synthetic control diagnostics. I will implement in-time placebo tests that assign the intervention to earlier dates, leave-one-out exercises that exclude influential donor units, sensitivity analyses using alternative donor pool definitions, and varying the length of the pre-treatment period. I will examine sensitivity to the ridge penalty parameter selected via cross-validation and report the balance between synthetic control weights

and the ridge-augmented bias correction term. I will also compare results to the classical synthetic control method (Appendix A) to assess the magnitude of the bias correction.

To distinguish trip rerouting from suppression or mode substitution, I will estimate treatment effects for the six cells adjacent to Friedrichstraße that were excluded from the donor pool. Attenuation of aggregate effects across the treated and adjacent cells would indicate spatial displacement; stable losses would suggest genuine trip suppression or mode shift.

I will also conclude with a discussion of policy implications, limitations related to Strava data coverage and representativeness, and external validity considerations for generalizing to other cycling infrastructure removals.

## References


[1] Malene Freudendal-Pedersen and Sven Kesselring. 9. Contested mobilities and the role of conflict in making sustainable cities. In Monika Grubbauer, Alessandra Manganelli, and Louis Volont, editors, *Conflicts in urban future-making*, pages 207–228. transcript Verlag, Bielefeld, 2024. ISBN 978-3-8394-7467-9. doi: doi:10.1515/9783839474679-009.

[2] David Harvey. Contested cities: Social process and spatial form. In Nick Jewson and Susanne Macgregor, editors, *Transforming cities: Contested governance and new spatial divisions*, pages 19–27. Taylor & Francis, 2018.

[3] Famke J. M. Mölenberg, Jenna Panter, Alex Burdorf, and Frank J. van Lenthe. A systematic review of the effect of infrastructural interventions to promote cycling: strengthening causal inference from observational data. *International Journal of Behavioral Nutrition and Physical Activity*, 16(1):93, October 2019. ISSN 1479-5868. doi: 10.1186/s12966-019-0850-1. URL *https://doi.org/10.1186/s12966-019-0850-1*.

[4] Marcel Moran, Malik Salman, and Takahiro Yabe. Causal Impacts of Protected Bike Lanes on Cycling Behavior with Demographic Disparities, July 2025. URL *http://arxiv.org/abs/2507.04936*. arXiv:2507.04936 [physics] version: 1.

[5] Maite Pellicer-Chenoll, Laura Antón-González, Israel Villarrasa-Sapiña, Jose Devís-Devís, Luis-Millán González, and Miquel Pans. Effects of building cycling infrastruc-

ture on bicycle use: Differences by gender through a longitudinal natural experiment study. *Research in Transportation Economics*, 110:101531, May 2025. ISSN 0739-8859. doi: 10.1016/j.retrec.2025.101531. URL *https://www.sciencedirect.com/science/article/pii/S0739885925000149*.

[6] Kyuhyun Lee and Ipek Nese Sener. Strava Metro data for bicycle monitoring: a literature review. *Transport Reviews*, 41(1):27–47, 2021. ISSN 0144-1647. doi: https://doi.org/10.1080/01441647.2020.1798558. URL *https://www.sciencedirect.com/science/article/pii/S0144164722000435*.

[7] Jaimy Fischer, Trisalyn Nelson, and Meghan Winters. Riding through the pandemic: Using Strava data to monitor the impacts of COVID-19 on spatial patterns of bicycling. *Transportation Research Interdisciplinary Perspectives*, 15:100667, 2022. ISSN 2590-1982. doi: https://doi.org/10.1016/j.trip.2022.100667. URL *https://www.sciencedirect.com/science/article/pii/S2590198222001270*.

[8] Luis F. Miranda-Moreno and Thomas Nosal. Weather or Not to Cycle: Temporal Trends and Impact of Weather on Cycling in an Urban Environment. *Transportation Research Record*, 2247(1):42–52, January 2011. ISSN 0361-1981. doi: 10.3141/2247-06. URL *https://doi.org/10.3141/2247-06*. Publisher: SAGE Publications Inc.

[9] Alberto Abadie, Alexis Diamond, and Jens Hainmueller. Synthetic control methods for comparative case studies: Estimating the effect of california's tobacco control program. *Journal of the American Statistical Association*, 105(490):493–505, 2010. doi: 10.1198/jasa.2009.ap08746. URL *https://doi.org/10.1198/jasa.2009.ap08746*. Publisher: Taylor & Francis tex.eprint: https://doi.org/10.1198/jasa.2009.ap08746.

[10] Eli Ben-Michael, Avi Feller, and Jesse Rothstein. The Augmented Synthetic Control Method. *Journal of the American Statistical Association*, 116(536):1789–1803, October 2021. ISSN 0162-1459. doi: 10.1080/01621459.2021.1929245. URL *https://doi.org/10.1080/01621459.2021.1929245*. Publisher: Taylor & Francis _eprint: https://doi.org/10.1080/01621459.2021.1929245.

# A Synthetic Control Diagnostics and Estimates

Results from the classical synthetic control estimator show larger pre-treatment discrepancies (Figure 3). The pre-treatment RMSPE is 987.34 trips per week. The average post-treatment effect is a reduction of 1,954.50 trips per week.

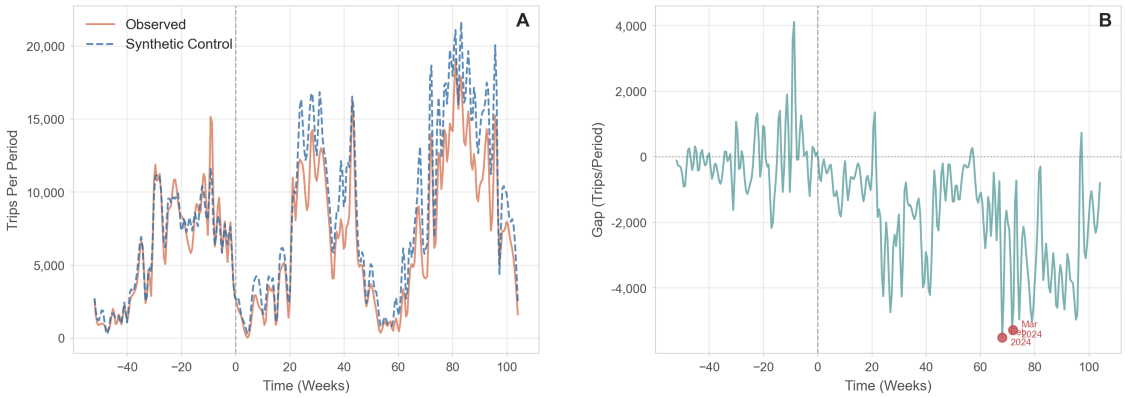


**Figure 3:** Observed and synthetic cycling activity in the treated hexagonal cell using the classical synthetic control estimator. Panel A shows weekly observed cycling trips and the synthetic control. Panel B plots the corresponding gap between observed and synthetic outcomes. The vertical dashed line marks the treatment date.

# B Donor Pool and Spatial Distribution of Weights

Figure 4 shows the spatial distribution of units used to construct the synthetic control. The treated hexagonal cell is highlighted. Donor units receiving positive weight are shaded according to their contribution, while excluded units are shown in outline only. Donor weights are concentrated in central Berlin, with no single donor dominating the synthetic control.

Table 1 reports observable characteristics of the treated unit and the five donor units receiving the largest weights in the synthetic control. Reported values summarize location, transport infrastructure, and commercial activity within each hexagonal cell.

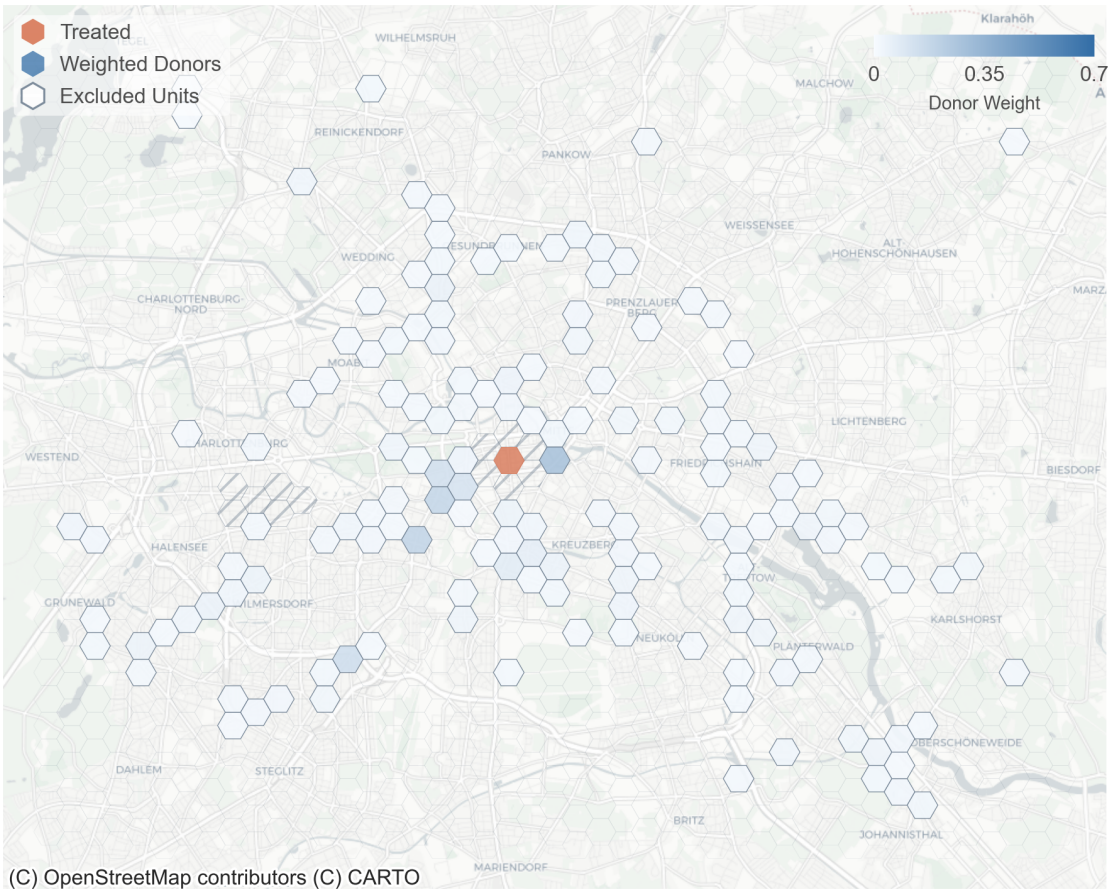


**Figure 4:** Spatial distribution of donor units used in the synthetic control. The treated hexagonal cell is highlighted in orange. Shaded cells indicate donor units receiving positive weight, with color intensity proportional to the assigned weight. Outlined cells denote excluded units.

**Table 1:** Treated Unit vs. Top 5 Donors

| Covariate | Treated | Donor 1 | Donor 2 | Donor 3 | Donor 4 | Donor 5 | Avg |
|---|---|---|---|---|---|---|---|
| Weight | — | 0.272 | 0.182 | 0.174 | 0.137 | 0.129 | — |
| Dist. to Center (m) | 3135 | 2037 | 7085 | 5732 | 11368 | 5332 | 5694 |
| Road Length (m) | 5844 | 5786 | 4743 | 6147 | 7935 | 5006 | 5863 |
| Bike Track (m) | 0 | 191 | 160 | 1630 | 729 | 1097 | 678 |
| Bike Lane (m) | 1 | 758 | 11 | 297 | 204 | 419 | 382 |
| U-Bahn Stops | 2 | 2 | 4 | 0 | 2 | 0 | 2 |
| S-Bahn Stops | 0 | 0 | 0 | 0 | 2 | 0 | 0 |
| Restaurants | 26 | 6 | 6 | 2 | 4 | 3 | 4 |
| Shops | 60 | 9 | 56 | 4 | 25 | 2 | 19 |